Fluorescent Lamp Modelling for Voltage Fluctuations

C. Carrillo, J. Cidrás

Abstract

The wide use of fluorescent lamps means their influence on the power system needs to be studied. A set of models that enables the evaluation of the electrical behaviour during steady state is presented in this paper. These models have different levels of complexity; starting by taking into account all the non-linearities of the lamp, passing through neglecting the non-linearities of the reactance, supposing the voltage wave shape of the tube to be square and, finally, treating the variations in the RMS source voltage as an steady-state phenomenon. The most complex model needs an iterative algorithm to get results, however analytical expressions can be achieved with the other models. Several situations can be analysed with the different models but special attention is paid to the sinusoidal voltage source and the modulated voltage source cases. Also, the study presented in this paper is focused on obtaining the waveshape of current, voltage and power in the tube. These waveforms allow the study of the normal steady-state functioning and the flicker phenomena. In this paper the simulation results for the above models in the two kinds of situations are shown. As a result, a performance test between the models is made and it is used to validate them.

1 Introduction

The flicker problem is well documented with reference to incandescent lamps. The international standards (e. g. IEC 60868) are based on this kind of lamp. However, fluorescent lamps are widely used and the flicker problem related to them is very important. Moreover, the physical mechanism of electrical energy conversion into light differs drastically between the two types of lamps. The fluorescent lamp is a discharge lamp that has a nonliner behaviour, and the incandescent lamp has a linear behaviour. The first one needs an arc inside the tube, the second one uses the Joule-heating process.

This paper is intended to cover the steady-state study of fluorescent lamps. Therefore a set of numerical and analytical simulation models is presented. The models have different degrees of complexity and accuracy.

First, the Complete Model [1] is presented. In this model, the most important non-linearities of the fluorescent lamp are represented. These are, the saturation and hysteresis effect on the reactance, and the arc phenomenon inside the tube. An iterative method is needed to analyse this approximation, then simpler models are proposed in order to get an easy method to analyse the fluorescent lamp through analytical expressions.

Approximate Model I is intended to be a simpler option. This simplification is achieved supposing the reactance to be linear. So, the saturation effect and the hysteresis effect are not taken into account in this model. Then analytical expressions have been achieved and the study is made quickly and easily.

A deeper simplification is made about the last model. The wave shape of the tube is supposed to be square and the resistance of the reactance is neglected. In this way the Approximate Model II is shown.

Finally, a last model is presented, the Approximate Model III [6]. This model comes from a simplification on the dynamic behaviour of the Approximate Model II, the RMS variations on the source voltage are treated as a static phenomenon. In this way the simplest expressions are reached.

All the above models are studied under two situations: the voltage source being a sinusoidal source and a modulated source. These situations help the study of the normal steady-state behaviour, i. e. harmonic analysis, and the flicker phenomenon. Special attention is paid to the current and power in the tube because they are closely related to the flicker and harmonic study.

The results for each Approximate Model are compared with the Complete Model in order to get a validation method. The loss of accuracy is the price for the simplicity, thus the Approximate Model III is expected to be the simplest and most inaccurate model.

2 Fluorescent Lamp Circuit

The main lamp elements are shown in the **Fig. 1**. These are: reactance, tube and starter.

This circuit has a strongly non-linear behaviour during the steady state, as shown see in **Fig. 2**. The arc inside the tube is the main cause of the distorted voltage shape. Thus the tube is the most important non-linearity in the circuit.

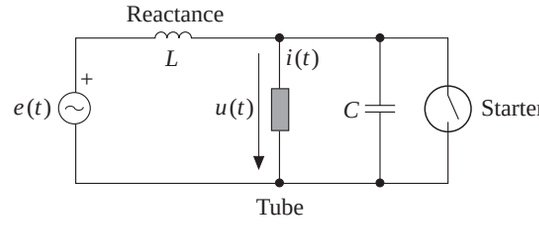

Fig. 1. Fluorescent lamp equivalent circuit

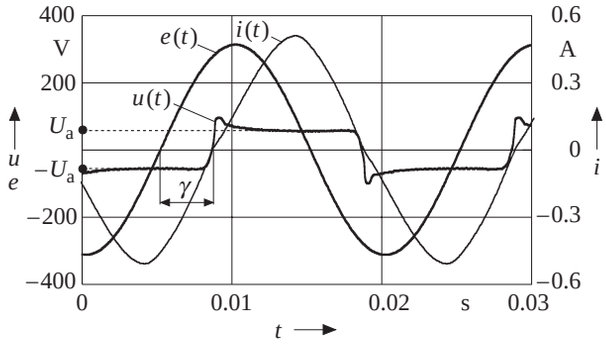

Fig. 2. Voltage and current waveforms

The hysteresis and the saturation in the iron core reactance are the other non-linearities taken into account for the fluorescent lamp study.

The starter is open during normal tube operation, so it has not been modelled.

In the following models all the parameters are obtained from the measurements on a typical 36-W tube (see Fig. 2).

3 Complete Model

In this part, the steps to get a simulation method for the fluorescent lamp are depicted [1].

Firstly, a description and modelling of the different elements are made. The study of reactance and tube have been emphasised, because these are the main non-linear elements.

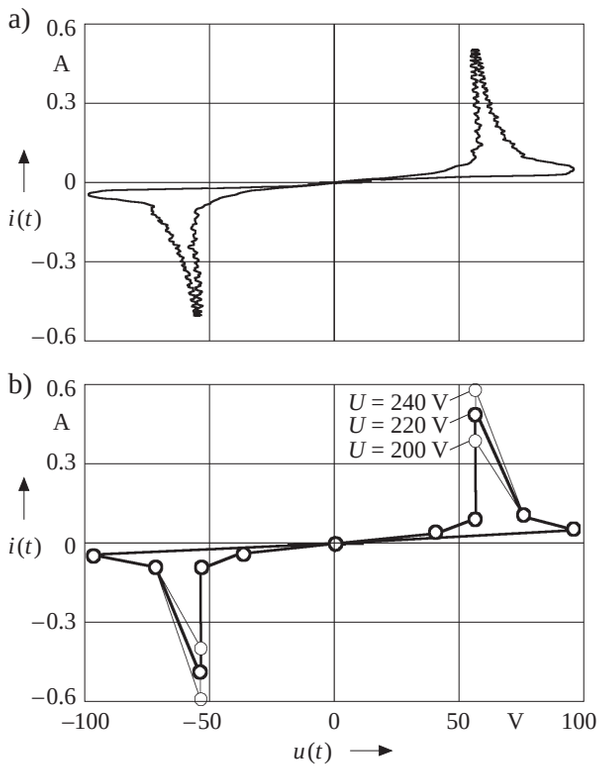

Fig. 3. Voltage-current characteristic of the fluorescent tube and its approximation
a) Measured (U = 220 V)
b) Approximate

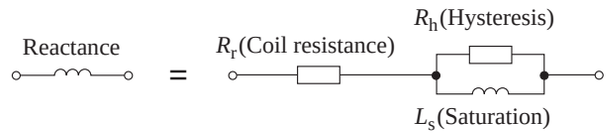

Fig. 4. Equivalent reactance model

The present non-linearities prevent a direct solution for a given voltage supply. Instead, an iterative approach is required for accurate derivation of currents and voltages in the lamp circuit. The power in the tube is the main result from the iterative analysis. The study of the flicker is based on this power, and this is the reason for its importance.

3.1 Model Description

In this section the tube and reactance model are depicted, because they are the main non-linearities of the lamp circuit.

As is shown in **Fig. 3**, the tube model is derived from a straight lines approximation of its voltage-current characteristic. In this way, an easy model for computer implementation is obtained.

The reactance is the following non-linear element for the modelling. The model must cover the coil resistance and the saturation and hysteresis effects in the iron core. A series resistance is used to model the coil resistance (**Fig. 4**). The saturation effect is modelled by a non-linear inductance, and it has the following equation [2]:

$$i(t) = k_1 \phi(t) + k_2 \phi^2(t), \tag{1}$$

where $\phi(t)$ is the flux in the iron core, $i(t)$ is the current across the inductance, and k_1, k_2 are constants.

Finally, a resistance in parallel with the non-linear inductance represents the hysteresis. Its value can be calculated from the equation [3]:

$$R_h = \phi_{max} \frac{\omega_1}{d_i}, \tag{2}$$

where ϕ_{max} is the maximum flux, ω_1 is the fundamental frequency of the source and d_i is one half of the hysteresis width at $\phi = 0$ (see **Fig. 5**). As a result, the model of the reactance is obtained.

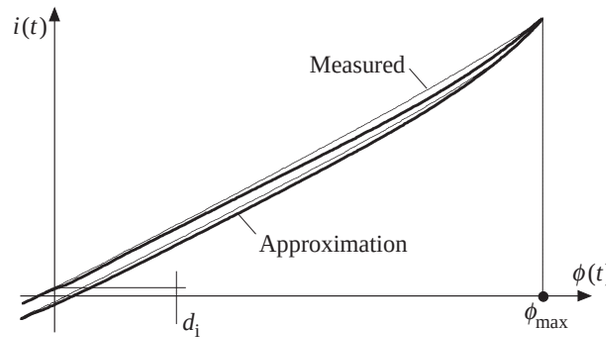

Fig. 5. Comparison between the hysteresis characteristic and its approximation

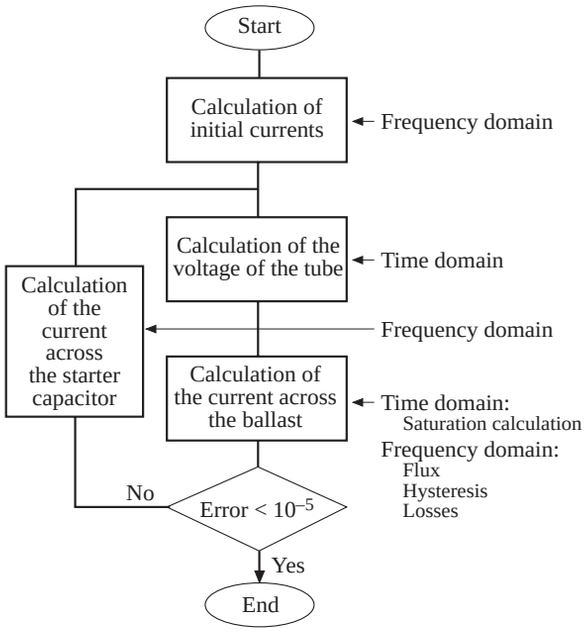

Fig. 6. Simulation flow diagram

3.2 Iterative Harmonic Analysis

Once the lamp has been modelled an iterative algorithm is used to derive the steady-state voltage and current wave shapes in the circuit. The algorithm called Iterative Harmonic Analysis [4] is illustrated in **Fig. 6**.

The Iterative Harmonic Analysis involves a hybrid technique which formulates the non-linear elements in the time domain (saturation and tube response), and the linear system in the frequency domain. The common current is used as the interface between the two systems in each iteration. Operations in the time domain and in the frequency domain are matched in order to obtain the steady-state response of the lamp circuit.

The current, instead of the voltage, has been chosen as an interface to improve the Iterative Harmonic Analysis rate of convergence. Since the tube voltage has a shape which is too distorted to be achieved with a iterative algorithm.

3.3 Power in the Tube

Any voltage or current can be calculated via Iterative Harmonic Analysis. However, the current and voltage in the tube are particularly interesting in order to obtain the electric power.

When there is a flicker phenomenon, this is closely connected with the electric power in the tube. Moreover, the human eye can detect oscillations between 0 Hz and 35 Hz, as an approximation of a Butterworth filter [5] with a cut frequency of 35 Hz. So the power variations between 0 Hz and 35 Hz are related to luminous flux variations that the eye can detect.

Therefore, the power $p(t)$ related to the visible luminous flux variations is calculated by filtering the instantaneous power $p_i(t)$ in the tube. The filter is an ideal low-pass one with a cut-off frequency of 35 Hz.

The power $P(t)$ could be weighted according to the flickermeter curve. However, the main purpose of this paper is to achieve models with ability to represent power fluctuations. So, the application of the mentioned curve is out of the scope of the paper.

4 Approximate Model I

With the Complete Model, the numeric calculation of the power in the tube can now be obtained. However, some simplifications on the model are needed to achieve an analytical power calculation. In the Approximate Model I two simplifications are made:

– The reactance is supposed to be linear. Thus, its model is an *R-L* combination, neglecting the hysteresis and saturation effects.

– The voltage wave shape of the tube is supposed to be constant. This simplification is more realistic when the source has small fluctuations. It must not be forgotten to take into account that in the tube, the phase shift between the current and voltage is equal to zero (see Fig. 2).

The equivalent lamp circuit with the above simplifications is shown in the **Fig. 7**. The circuit behaviour follows the differential equation:

$$e(t) - u(t) = R\,i(t) + L\,\frac{\mathrm{d}i(t)}{\mathrm{d}t}, \tag{3}$$

where $e(t)$ is the source voltage. One condition for the equation solution is the zero value for the phase shift between $i(t)$ and $u(t)$.

If the phase reference is the current or voltage in the tube, the harmonic spectrum of $u(t)$ is constant. However, the usual phase reference is the voltage source, so the harmonic factoring is:

$$u(t) = \sum_{n=0}^{\infty} U_n \sin(n\,\omega_1 t + \theta_n - n\gamma), \tag{4}$$

where ω_1 is the fundamental frequency of the source, U_n and ϕ_n are constant values because of the above simplifications and γ is the phase shift between the source voltage $e(t)$ and voltage in the tube $u(t)$ (or the current across the tube $i(t)$).

As is shown in eq. (4), the voltage $u(t)$ only depends on the phase shift γ.

4.1 Sinusoidal Voltage Source

The usual and simplest situation in which to study the fluorescent lamp behaviour is when the voltage source is pure sinusoidal, thus:

$$e(t) = \sqrt{2}\,U \sin(\omega_1 t), \tag{5}$$

where U is the RMS source voltage.

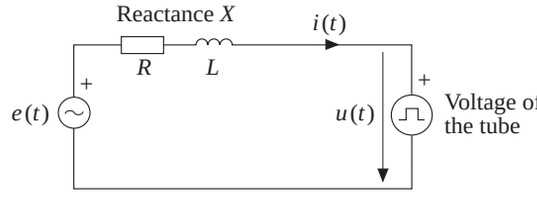

Fig. 7. Approximate Model I (U_n constant and $X = R + L$)

The frequency domain is more appropriate in order to study the steady-state behaviour. So, eq. (5) gives:

$$\underline{I}(\omega) = \frac{\underline{E}(\omega) - \underline{U}(\omega)}{R + \mathrm{j}\omega L}, \tag{6}$$

where $\underline{E}(\omega)$ and $\underline{U}(\omega)$ are the Fourier transforms of $e(t)$ (see eq. (5)) and $u(t)$ (see eq. (4)), and R-L are the values for the reactance simplification.

The solution of eq. (6) gives an expression for the current:

$$i(t) = \frac{-\sqrt{2}\,U}{Z_c(\omega_1)}\cos\left(\omega_1 t - \theta_c(\omega_1)\right) + \sum_{n=1}^{\infty}\frac{U_n}{Z_c(n\omega_1)}\cos\left(n\omega_1 t - \theta_c(n\omega_1) + \theta_n - n\gamma\right), \tag{7}$$

where $Z_c(\omega)$ and $\theta_c(\omega)$ represent the module and phase shift of the L-R impedance. Their expressions are:

$$Z_c(\omega) = \sqrt{R^2 + (\omega L)^2}, \qquad \theta_c(\omega) = -\frac{\pi}{2} + \tan^{-1}\left(\frac{\omega L}{R}\right). \tag{8}$$

At this moment, the parameter γ can be obtained and, in this way, the voltage $e(t)$ of eq. (4) and current $i(t)$ of eq. (7) are completely known. For this purpose the zero shift condition is used:

$$i\left(\frac{\gamma}{\omega_1}\right) = 0. \tag{9}$$

Substitution of eq. (9) in eq. (7) results in:

$$\gamma = \theta_c(\omega_1) + \cos^{-1}\left[\sum_{n=1}^{\infty}\frac{U_n}{\sqrt{2}\,U}\frac{Z_c(\omega_1)}{Z_c(n\omega_1)}\cos\left(\theta_n - \theta_c(n\omega_1)\right)\right]. \tag{10}$$

The procedure shown in Section 3.3 is used in order to get the power in the tube:

$$P_0 = \frac{\sqrt{2}\,U_1}{2Z_c(\omega_1)}\cdot\left[U\sin\left(\gamma - \theta_1 - \theta_c(\omega_1)\right) + U_1\sin\left(\theta_c(\omega_1)\right)\right]. \tag{11}$$

4.2 Modulated Voltage Source

In order to study the flicker phenomenon in the fluorescent lamp, we assume that the supply voltage is modulated by sinusoidal voltage of a lower frequency:

$$e(t) = \sqrt{2}\,U\left(1 - \frac{a}{2} + \frac{a}{2}\cos(\Omega t)\right)\sin(\omega_1 t), \tag{12}$$

where Ω is the modulation frequency ($\Omega \le \omega_0/2$) and a is the modulation factor ($0 < a < 0.2$).

Proceeding as in the previous section the following expression for the current is achieved:

$$\begin{aligned} i(t) = {} & \frac{-\sqrt{2}\,U(1 - a/2)}{Z_c(\omega_1)}\cos\left(\omega_1 t - \theta_c(\omega_1)\right) \\ & - \frac{\sqrt{2}\,aU}{4}\frac{\cos\left((\omega_1 + \Omega)t - \theta_c(\omega_1 + \Omega)\right)}{Z_c(\omega_1 + \Omega)} \\ & - \frac{\sqrt{2}\,aU}{4}\frac{\cos\left((\omega_1 - \Omega)t - \theta_c(\omega_1 - \Omega)\right)}{Z_c(\omega_1 - \Omega)} \\ & + \sum_{n=1}^{\infty}\frac{U_n}{Z_c(n\omega_1)}\cos\left(n\omega_1 t + \theta_n - n\gamma - \theta_c(n\omega_1)\right). \end{aligned} \tag{13}$$

At this point, the use of the condition $i(\gamma/\omega_1) = 0$ results in:

$$\begin{aligned} f(\gamma) = i(\gamma/\omega_1) = {} & \frac{-\sqrt{2}\,U(1 - a/2)}{Z_c(\omega_1)}\cos\left(\gamma - \theta_c(\omega_1)\right) \\ & - \frac{\sqrt{2}\,aU}{4}\frac{\cos\left(\frac{\omega_1 + \Omega}{\omega_1}\gamma - \theta_c(\omega_1 + \Omega)\right)}{Z_c(\omega_0 + \Omega)} \\ & - \frac{\sqrt{2}\,aU}{4}\frac{\cos\left(\frac{\omega_1 - \Omega}{\omega_1}\gamma - \theta_c(\omega_1 - \Omega)\right)}{Z_c(\omega_0 - \Omega)} \\ & + \sum_{n=1}^{\infty}\frac{U_n}{Z_c(n\omega_1)}\cos\left(\theta_n - \theta_c(n\omega_1)\right) = 0. \end{aligned} \tag{14}$$

The above non-linear equation must be solved by an iterative method. The well-known Newton-Raphson method is chosen, which means that, before calculation, the following conditions are needed:

– The derivative , for which the equation is:

$$\begin{aligned} f'(\gamma) = \frac{\mathrm{d}f(\gamma)}{\mathrm{d}\gamma} = {} & \frac{\sqrt{2}\,U(1 - a/2)}{Z_c(\omega_1)}\sin\left(\gamma - \theta_c(\omega_1)\right) \\ & + \frac{\sqrt{2}\,aU}{4Z_c(\omega_1 + \Omega)}\frac{\omega_1 + \Omega}{\omega_1} \\ & \cdot\cos\left(\frac{\omega_1 + \Omega}{\omega_1}\gamma - \theta_c(\omega_1 + \Omega)\right) \\ & + \frac{\sqrt{2}\,aU}{4Z_c(\omega_1 - \Omega)}\frac{\omega_1 - \Omega}{\omega_1} \\ & \cdot\cos\left(\frac{\omega_1 - \Omega}{\omega_1}\gamma - \theta_c(\omega_1 - \Omega)\right). \end{aligned} \tag{15}$$

– An initial guess for γ. This value is calculated from eq. (14), supposing $a = 0$ and the a Newton-Raphson algorithm is applied.

The power in the tube is:

$$p(t) = P_0 + P_\Omega(t), \tag{16a}$$

$$P_0 = \frac{\sqrt{2}\,U_1}{2Z_c(\omega_1)}\left[U(1 - a/2)\sin\left(\gamma - \theta_1 - \theta_c(\omega_1)\right) + U_1\sin\left(\theta_c(\omega_1)\right)\right], \tag{16b}$$

$$P_{\Omega}(t) = \frac{-\sqrt{2}\,a\,UU_1}{8}\,\frac{\sin\left(\Omega t + \theta_1 - \gamma + \theta_c(\omega_1 - \Omega)\right)}{Z_c(\omega_1 - \Omega)} + \frac{-\sqrt{2}\,a\,UU_1}{8}\,\frac{\sin\left(\Omega t - \theta_1 + \gamma - \theta_c(\omega_1 + \Omega)\right)}{Z_c(\omega_1 + \Omega)}, \tag{16c}$$

where P_0 is the mean power, and $P_{\Omega}(t)$ is the alternating component.
The fluctuations that the eye can see are represented by $P_{\Omega}(t)$, whose fundamental frequency is simply Ω and whose amplitude is P_{Ω}.

5 Approximate Model II

In order to obtain simpler analytic power and current expressions, more simplifications have been be made on the previous model. In this model the voltage of the tube is supposed to be a square wave. This wave has a zero phase shift with regard to the current, as is shown in **Fig. 8**. The coil resistance is neglected in order to achieve a higher degree of simplification.

The square voltage in the tube is:

$$u(t) = \frac{4U_a}{\pi}\sum_{n=0}^{\infty}\frac{\sin\left[(2n+1)(\omega_1 t - \gamma)\right]}{2n+1}, \tag{17}$$

where U_a is the maintenance voltage of the arc inside the tube (see Fig. 2).

The above expression comes from Fourier factoring of a square wave whose extreme values are Ua and -Ua. The resulting wave forms after the new simplifications are shown in **Fig. 9**.

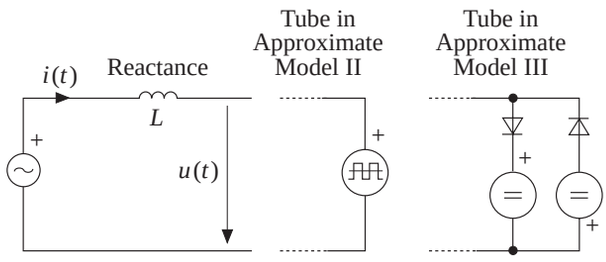

Fig. 8. Approximate Model II and Approximate Model III

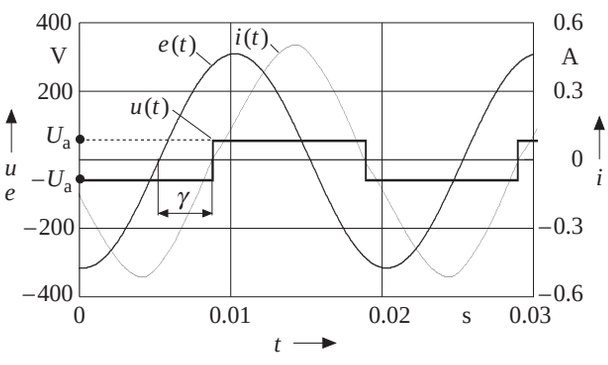

Fig. 9. Voltage and current waveforms in the simplified circuit

5.1 Sinusoidal Voltage Source

If the source voltage expression is eq. (5), an expression for the current is reached with similar steps to those in previous sections:

$$i(t) = \frac{-\sqrt{2}\,U}{\omega_0 L}\cos(\omega_1 t) + \frac{4U_a}{\pi\omega_0 L}\sum_{n=1}^{\infty}\frac{\cos\left[(2n+1)(\omega_1 t - \gamma)\right]}{(2n+1)^2}. \tag{18}$$

The phase shift between $i(t)$ (or $u(t)$) and $e(t)$ is:

$$\cos\gamma = \frac{U_a\,\pi}{2\sqrt{2}\,U}. \tag{19}$$

So, the power is:

$$P_0 = \frac{2\sqrt{2}\,UU_a}{\pi\,\omega_1 L}\sin\gamma. \tag{20}$$

5.2 Modulated Voltage Source

When the source voltage has the expression shown in eq. (12), then the current is:

$$i(t) = \frac{-\sqrt{2}\,U(1-a/2)}{\omega_1 L}\cos(\omega_1 t) - \frac{\sqrt{2}\,a\,U}{4L}\left[\frac{\cos(\omega_1+\Omega)t}{\omega_1+\Omega} + \frac{\cos(\omega_1-\Omega)t}{\omega_1-\Omega}\right] + \frac{4U_a}{\pi\,\omega_1 L}\sum_{n=0}^{\infty}\frac{\cos\left[(2n+1)(\omega_1 t - \gamma)\right]}{(2n+1)^2}. \tag{21}$$

The Newton-Raphson algorithm is used again in order to obtain the phase shift γ. The following expressions are used:

$$f(\gamma) = \frac{-\sqrt{2}\,U(1-a/2)}{\omega_1 L}\cos\gamma - \frac{\sqrt{2}\,a\,U}{4L}\left[\frac{\cos\left[(\omega_1+\Omega)\frac{\gamma}{\omega_1}\right]}{\omega_1+\Omega} + \frac{\cos\left[(\omega_1-\Omega)\frac{\gamma}{\omega_1}\right]}{\omega_1-\Omega}\right] + \frac{U_a\,\pi}{2\omega_1 L} = 0; \tag{22}$$

$$f'(\gamma) = \frac{\mathrm{d}\,f(\gamma)}{\mathrm{d}\gamma} = \frac{\sqrt{2}\,U}{\omega_1 L}\left(1 - \frac{a}{2} + \frac{a}{2}\cos\left(\frac{\Omega}{\omega_1}\gamma\right)\right)\sin\gamma. \tag{23}$$

So the power in the tube is:

$$p(t) = P_0 + P_{\Omega}(t), \tag{24a}$$

$$P_0 = \frac{2\sqrt{2}\,UU_a(1-a/2)}{\pi\,\omega_1 L}\sin\gamma, \tag{24b}$$

$$P_{\Omega}(t) = -\frac{\sqrt{2}\,a\,UU_{\mathrm{a}}}{2\pi L}\left[\frac{\sin(\Omega t-\gamma)}{\omega_1-\Omega}-\frac{\sin(\Omega t+\gamma)}{\omega_1+\Omega}\right]. \tag{24c}$$

where P_0 is the mean power in the tube and $P_{\Omega}(t)$ is the alternating power in the tube.

6 Approximate Model III

Another simplification level is when the modulation frequency is very low ($\Omega \ll 0$). Then the voltage fluctuations can be considered as a static phenomenon. This simplification is referred to as Approximate Model III [6].

6.1 Sinusoidal Voltage Source

With the source as sinusoidal the results are the same as those shown in eq. (20) for Approximate Model II.

6.2 Modulated Voltage Source

When a modulated voltage source is applied to this model, the power can be obtained by simply substituting eq. (12) in eq. (20) which results in:

$$p(t) = \frac{1}{\pi\omega_1 L}\sqrt{8U^2U_{\mathrm{a}}^2\left(1-\frac{a}{2}+\frac{a}{2}\cos(\Omega t)\right)^2-\pi^2U_{\mathrm{a}}^4}\,. \tag{25}$$

6.3 Simulation

The simplicity of the Approximate Model III allows an easy way to get a simulation equivalent. This equivalent is depicted in Fig. 8.

7 Results

All the models have been simulated under several modulation frequencies Ω = 3.125 Hz, 6.25 Hz, 12.5 Hz 25.0 Hz, and modulation factors a = 0.00 p.u., 0.05 p.u., 0.10 p.u., 0.15 p.u., 0.20 p.u. In the following figures the results from these simulations are represented.

8 Conclusions

The results from measurements (Measured Power) on a typical 36-W tube under the same conditions as the simulation models are included (**Fig. 10** and **Fig. 11**).

The analysis of the simulation results presented in the above-mentioned figures leads to the following conclusions:

– As can be shown in Fig. 10, the mean power (P_0) is the most important power component. The second one is the component $P_{\Omega}(t)$ whose oscillation frequency is Ω. Different terms of frequency are present only in the Complete Model and in the Measured Power, but they can be neglected.

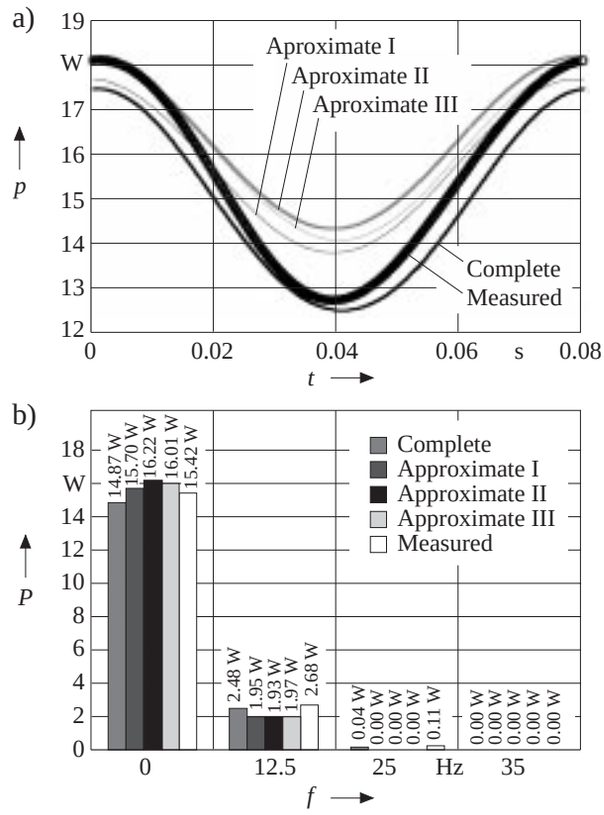

Fig. 10. Power with the different models (Ω = 12.5 Hz; a = 0.2)
a) Time-domain power
b) Frequency-domain power (0 Hz … 35 Hz)

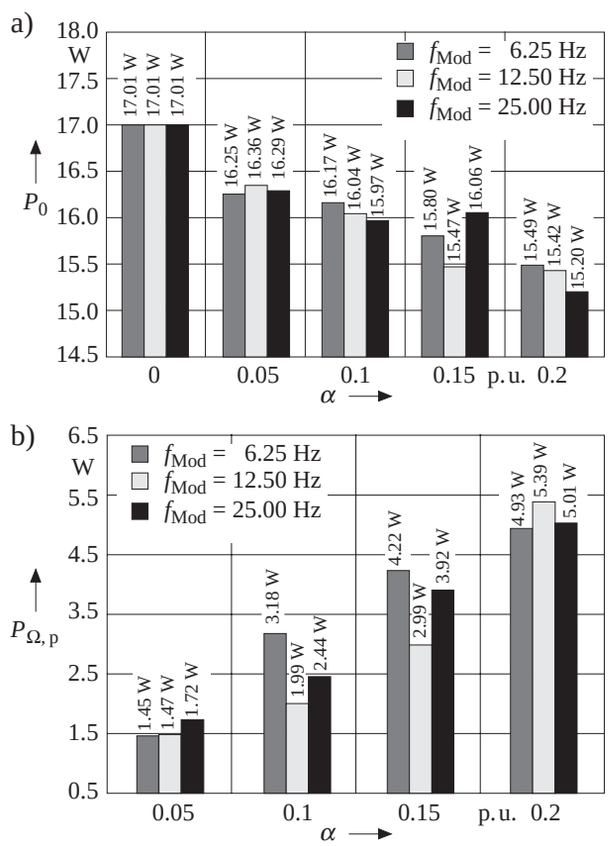

Fig. 11. Measured power
a) Time-domain power
b) Frequency-domain power (0 Hz … 35 Hz)

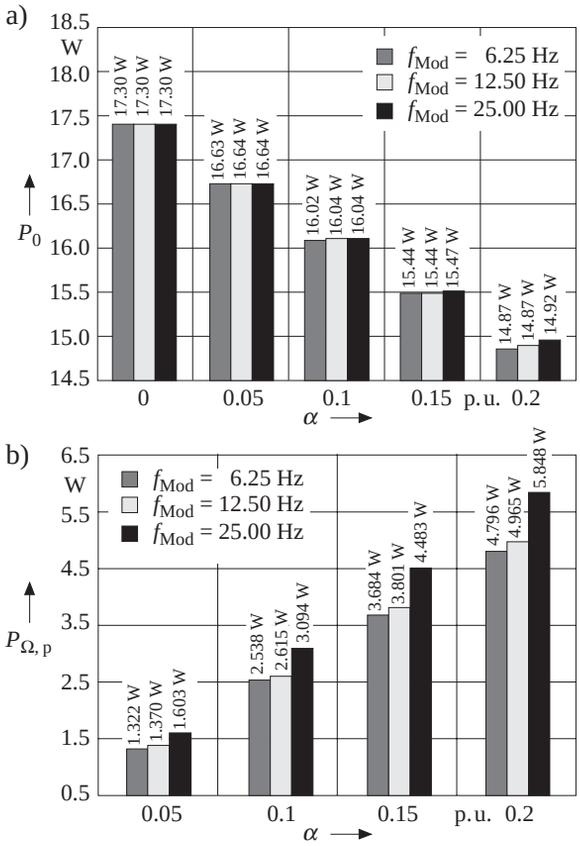

Fig. 12. Mean and alternating power with the Complete Model
a) Time-domain power
b) Frequency-domain power (0 Hz … 35 Hz)

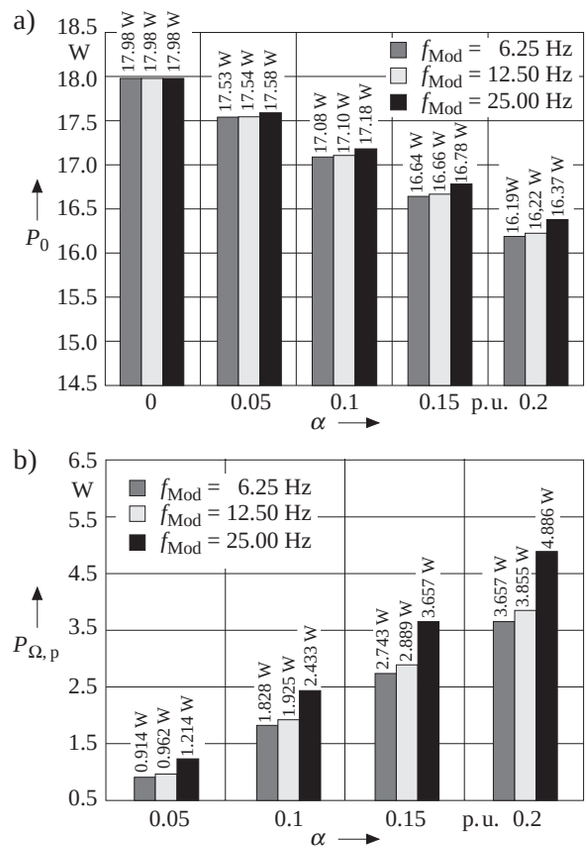

Fig. 14. Mean and alternating power with Approximation II
a) Time-domain power
b) Frequency-domain power (0 Hz … 35 Hz)

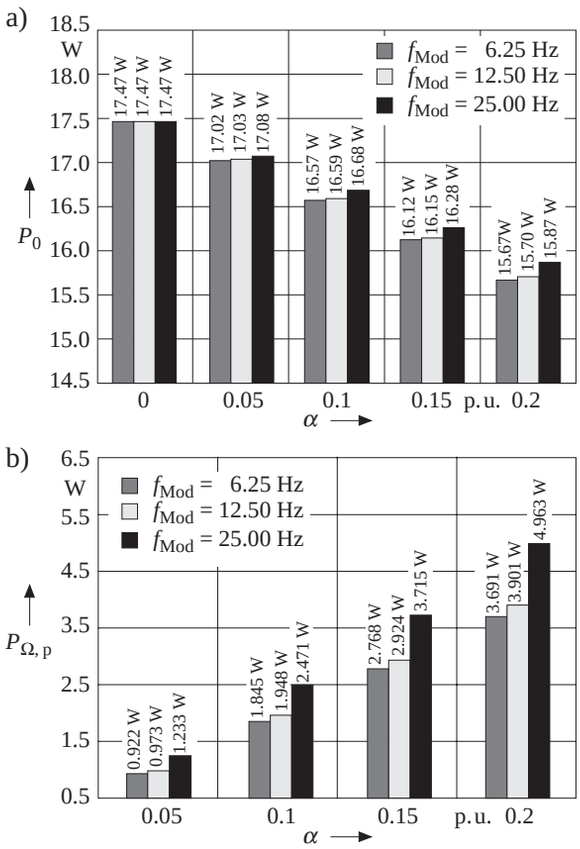

Fig. 13. Mean and alternating power with Approximation I
a) Time-domain power
b) Frequency-domain power (0 Hz … 35 Hz)

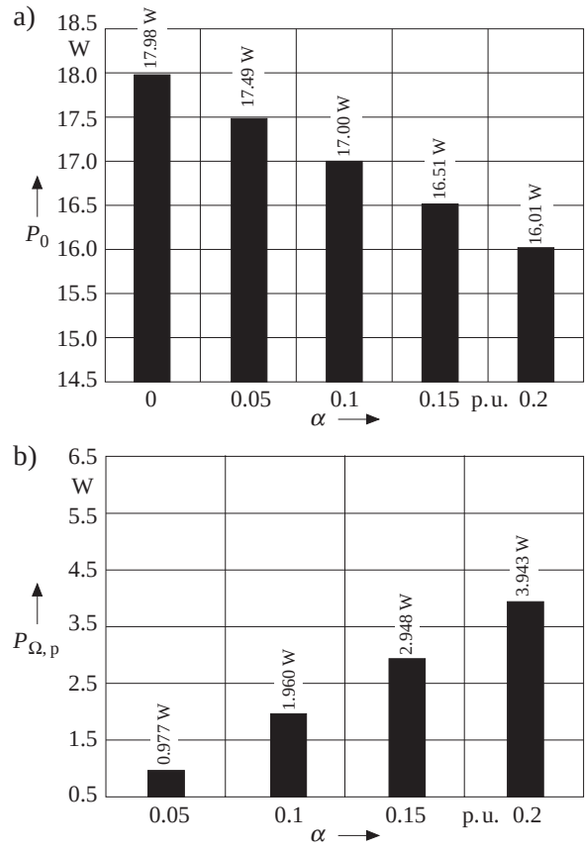

Fig. 15. Mean and alternating power with Approximation III
a) Time-domain power
b) Frequency-domain power (0 Hz … 35 Hz)

Mean power	$\alpha(\Omega)$	Approximation error
Complete	−12.2397	0.2028 %
Approximation I	−7.9597	0.0179 %
Approximation II	−8.0175	0.0194 %
Approximation III	−9.8069	0.0099 %
Alternating power	$\beta(\Omega)$	**Approximation error**
Complete	30.0579	2.5150 %
Approximation I	24.7630	0.1654 %
Approximation II	24.3783	0.1666 %
Approximation III	19.6559	0.2424 %
Ω = 12.5 Hz and a = 0.2 p.u.		

Tab. 1. Approximation by the Least-Square Method of the Mean and Alternating Power Coefficients $\alpha(\Omega)$ and $\beta(\Omega)$

– In the simulation models, the mean power P_0 and the alternating power amplitude P_Ω have linear dependence on the modulation factor a (see **Fig. 12**, **Fig. 13**, **Fig. 14** and **Fig. 15**). If the modulation frequency Ω is constant then the mean power and the alternating power amplitude are:

$$P_0 = P_0\big|_{a=0} + \alpha(\Omega)\,a\,, \quad P_{\Omega,\mathrm{p}} = \beta(\Omega)\,a, \tag{26}$$

where $P_0|_{a=0}$ is the mean power (with $a = 0$), P_0 is the mean power and $P_{\Omega,\mathrm{p}}$ is the alternating power amplitude. The coefficients $\alpha(\Omega)$, $\beta(\Omega)$ are calculated via the Least-Square Method, and the results are shown in **Tab. 1**. This linear behaviour in not so clear in the Measured Power (Fig. 11).

– The mean power P_0 decreases with the modulation factor and increases with the modulation frequency. Whereas the alternating power amplitude increases with the modulation factor and with the modulation frequency.

– When low values of modulation factor and modulation frequency are used, the lowest differences between the Approximate models and Complete Model are achieved. However, in all simulations the Complete Model has had the lowest error with relation to the Measured Power.

– The difference between the models and the measurements are not negligible because of the dependence on the frequency and amplitude of characteristic of the tube (see Fig. 3).

– *In summary*

  – The lamp behaviour under voltage fluctuations cannot be derived from the steady state with sinusoidal voltage.

  – High errors are obtained using the different models, however, the complete model is the nearest to the tube behaviour.

9 List of Symbols

9.1 Symbols

t	time
ω	frequency
$\underline{F}(\omega)$	Fourier transform of $f(t)$
K	modulation factor
Ω	modulation frequency
u, U	voltage in the tube
U_a	maintenance voltage of the arc inside the tube
e, E	source voltage
i, I	current across the tube
p, P	power composed by frequency components between 0 Hz and 35 Hz of the instantaneous power $p_\mathrm{i}(t)$
p_i	power before filtering
ϕ	flux in the iron core of the reactance
γ	phase shift between the source voltage e and the voltage in the tube u
$f(\gamma)$	current across the tube when $t = \gamma/\omega_0$
Z_c, θ_c	module and phase of the reactance impedance
d_i	one half of the hysteresis when $\phi(t) = 0$
k_1, k_2	saturation curve constants
X	reactance
R	coil resistance of the reactance
R_h	resistance that represents the hysteresis in the reactance
L	inductance for the reactance
n	harmonic order

9.2 Subscripts

0	mean power
1	fundamental component
n	n-th harmonic
s	with saturation
Ω	alternating power
k	k-th iteration in the Newton-Raphson algorithm
max	maximum
p	peak value or amplitude

9.3 Abbreviations

IEC	International Electrotechnical Commission
RMS	root mean square

References

[1] *Cidrás, J.; Carrillo, C.; Arrillaga, J.:* An Iterative Algorithm for the Analysis of the Harmonic Currents Produced by Fluorescent Lamps. 7th Int. Conf. on Harmon. and Quality of Power (ICHQP), Las Vegas/USA 1996, Proc. pp. 687–692

[2] *Watson, N.; Robbies, A.; Arrillaga, J.:* Representing Transformer Saturation in Iterative Harmonic Analysis. Int. Conf. on Harmon. Power Syst. (ICHPS-VI), Bologna /Italy 1994, Proc. pp. 318–324

[3] Electromagnetic Transient Program (EMTP)/ATP Reference manual. Leuven Center, Belgium,1987

[4] *Arrillaga, J.; Watson, N. R.; Eggleston, J. F.; Callaghan: C. D.:* Comparisons of Steady and Dynamic Models for the Calculation of AC/DC System Harmonics. Proc. of IEE 134-C (1987) no. 1, pp. 31–37

[5] IEC/TR2 60868 (1986-09): Flickermeter – Functional and design specifications. Offenbach · Berlin/Germany: VDE VERLAG, 1986

[6] *Emanuel, E.; Peretto, L.:* The Response of Fluorescent Lamp with Magnetic Ballast to Voltage Distortion. IEEE Trans. on Power Delivery PWRD-12 (1997) no. 1, pp. 289–295

Manuscript received on August 5, 1999

The Authors

Camilo Carrillo (1967) received his degree in electrical engineering from the University of Vigo (Spain) in 1992. Since these year he has been a lecturer in the Department of Electrical Engineering. His main fields of research are: harmonics, flicker and wind energy systems. (Dpto. Enxeñería Eléctrica, ETSEIM, Universidade de Vigo, Lagoas Marcosende S/n, 36200 Vigo /Spain, Phone: + 34 9 86 81 39 12, Fax: + 34 9 86 81 21 73, E-mail: carrillo@uvigo.es)

José Cidrás (1957) has received his degree in Electrical Engineering from the University of Las Palmas de G.C. (Spain). He obtained a PhD in electrical engineering from the University of Santiago (Spain) in 1987. He is professor and head of the Department of Electrical Engineering of the University of Vigo (Spain), and leads some investigation projects on wind energy, photovoltaics and planning of power systems. He is a Member of IEEE. (Dpto. Enxeñería Eléctrica, ETSEIM, Universidade de Vigo, Lagoas Marcosende s/nº, 36200 Vigo/Spain, Phone: + 34 9 86 81 21 21, Fax: + 34 9 86 81 21 73, E-mail: jcidras@uvigo.es)